A set of new observables in the process $e^+e^- \to ZHH$.

Junya Nakamura
Institut für theoretische Physik, Universität Tübingen, Germany
junya.nakamura@itp.uni-tuebingen.de

arXiv:1710.07251v2 [hep-ph] 27 Oct 2017

Abstract

Consequences of non-standard Higgs couplings in the final-state distributions of the process $e^+e^- \to ZHH$ are studied. We derive an analytic expression for the differential cross section, which has in the most general case 9 non-zero functions. These functions are the coefficients of 9 angular terms, depend on the Higgs couplings, and can be experimentally measured as observables. Symmetry properties of these 9 functions are carefully discussed, and they are divided into 4 categories under CP and CP$\widetilde{\mathrm{T}}$. The relations between our observables and the observables which exist in the literature are also clarified. We numerically study the dependence of our observables on the parameters in an effective Lagrangian for the Higgs couplings. It is shown that these new observables depend on most of the effective Lagrangian parameters in different ways from the total cross section. A benefit from longitudinally polarized e^+e^- beams is also discussed.

1 Introduction

One of the main targets of experiments at future e^+e^- colliders is the measurement of the trilinear self-coupling λ_H of the Higgs boson [1–5]. The process $e^+e^- \to ZHH$ is expected to be the best reaction to measure λ_H in the earlier stage of experiments [6–16] (i.e. the center-of-mass energy $\sqrt{s} \simeq 500$ GeV) for the discovered Higgs boson with mass $\simeq 125$ GeV [17, 18]. The process is sensitive to the couplings $HHZZ$ [19] and $HHZ\gamma$, too, which cannot be accessed through single Higgs boson production processes such as $e^+e^- \to ZH$.

Due to its importance, many authors have investigated the process. The total cross section in the standard model (SM) was calculated for the first time in ref. [19]. This work was followed by several studies [20, 21]. These papers numerically calculated various distributions of the final particles, too. The one-loop radiative corrections to the process were calculated in refs. [22, 23]. The total cross section in the minimal supersymmetric extension of the SM [24–28], that in composite Higgs models [29, 30] and that in other several new physics models [31] have also been studied in detail. Refs. [25–27] included the analytic form of the 2 Higgs energy distributions. The accuracy of measuring λ_H through the process $e^+e^- \to ZHH$ at future e^+e^- colliders has been studied in refs. [6–16] by assuming that all the other couplings are the SM values. The expected constrains on several parameters (including parameters which affect λ_H) in an effective Lagrangian have been discussed in refs. [32–35]. Ref. [33] included the analytic form for the invariant mass distribution of the 2 Higgs bosons.

Most of the above studies, however, restricted themselves to the total cross section as inputs from the experiments. This will not be a problem, if one intends to determine only one parameter such as λ_H. However, if one intends to determine more than one parameters at the same time as studied in refs. [32–35], measuring only the total cross section is not enough and one needs to consider other observables such as the invariant mass distribution of the 2 Higgs bosons [33, 34]. The purpose of this paper is to introduce such observables in a rather different way. We find 9 observables as the coefficients of 9 angular terms in the differential cross section, one of which is directly related to the total cross section. The other 8 observables have not been studied in the literature. Symmetry properties of the 9 observables are clarified, and they are divided into 4 categories under CP and CP$\widetilde{\mathrm{T}}$ [36]: 4 even-even, 1 even-odd, 2 odd-even and 2 odd-odd. The CP-odd observables directly measure CP non-conservation and the CP$\widetilde{\mathrm{T}}$-odd observables

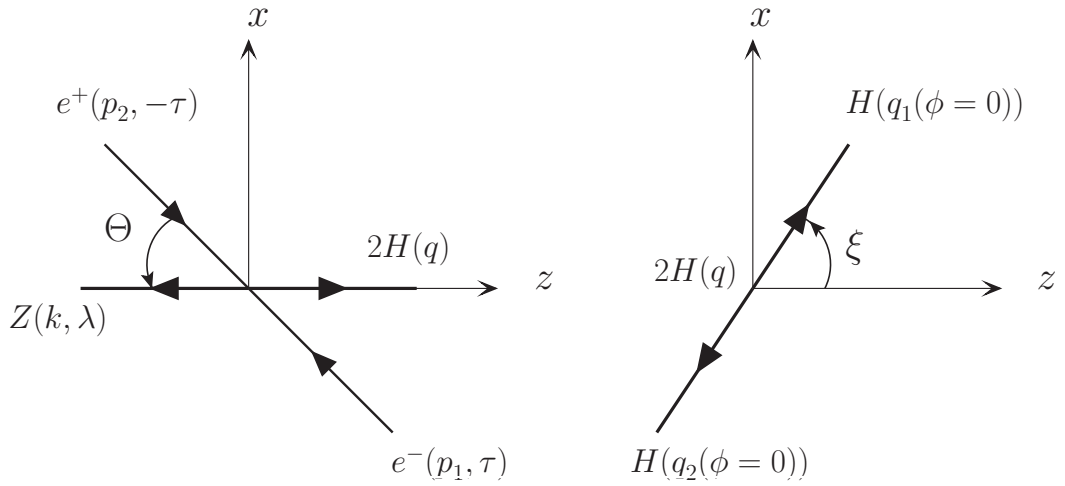


Figure 1: *Left*: The coordinate system in the c.m. frame of the colliding e^+e^- beams. The four-momentum and helicity of each particle are shown in parenthesis. A single object as the sum of the two Higgs bosons is represented by $2H$, whose four-momentum is q^μ. The direction of $\vec{q}$ is chosen as the z-axis and the $\vec{p}_1 \times \vec{k}$ direction as the y-axis. *Right*: The coordinate system in the c.m. frame of the two Higgs bosons (i.e. the rest frame of q^μ). The parametrization of the four-momenta in this frame is given in eq. (2.2).

re-scattering effects. To our knowledge, any CP-odd and/or CP$\widetilde{\text{T}}$-odd observables in this process have not been constructed so far.

This paper is organized as follows. In Section 2, we explain kinematics of the process $e^+e^- \to ZHH$. In Section 3, we give an analytic expression for the differential cross section. The differential cross section has 9 non-zero functions in the most general case and these 9 functions can be measured experimentally. We re-derive the analytic forms of the observables which exist in the literature and have been widely used, such as the invariant mass distribution of the 2 Higgs bosons. We show that all of these observables are directly related to just one of our 9 functions. The analytic form of the Z boson polar angle distribution is also derived. In Section 4, the symmetry properties of the 9 functions are studied. In Section 5, we form observables in terms of our 9 functions and numerically study the dependence of these observables on the parameters in an effective Lagrangian for the Higgs couplings. We show that our new observables depend on most of the effective Lagrangian parameters in different ways than the total cross section. It is also shown that the sensitivity of the CP$\widetilde{\text{T}}$-odd observable can be significantly enhanced by means of longitudinally polarized e^+e^- beams. Section 6 summarizes our findings.

2 Kinematics

Our coordinate system in the center-of-mass (c.m.) frame of the colliding e^+e^- beams is described in Figure 1 [1]. The four-momentum and helicity of each particle are shown in parenthesis. A single object as the sum of the two Higgs bosons is represented by $2H$, whose four-momentum is q^μ. We choose the direction of $\vec{q}$ as the z-axis and the $\vec{p}_1 \times \vec{k}$ direction as the y-axis. The scattering $p_1 + p_2 \to k + q$ takes place in the x-z plane. The polar angle of the Z boson from the electron momentum direction is denoted by Θ. Because we neglect the $e^\pm$ masses *and* e^- and e^+ always construct a four-vector in our process, the helicity of e^+ is always opposite to that of e^-. In this coordinate system, the four-momenta can be parametrized as follows:

$$\begin{aligned}
p^\mu &\equiv (p_1+p_2)^\mu = (E,0,0,0),\\
p_1^\mu &= \frac{E}{2}\big(1,\sin\Theta,0,-\cos\Theta\big),\\
p_2^\mu &= \frac{E}{2}\big(1,-\sin\Theta,0,\cos\Theta\big),\\
k^\mu &= (w,0,0,-l),\\
q^\mu &= (q_1+q_2)^\mu = (E-w,0,0,l),
\end{aligned} \tag{2.1}$$

[1] Figures 1, 2, 3, 4 are drawn by using the program JaxoDraw [37].

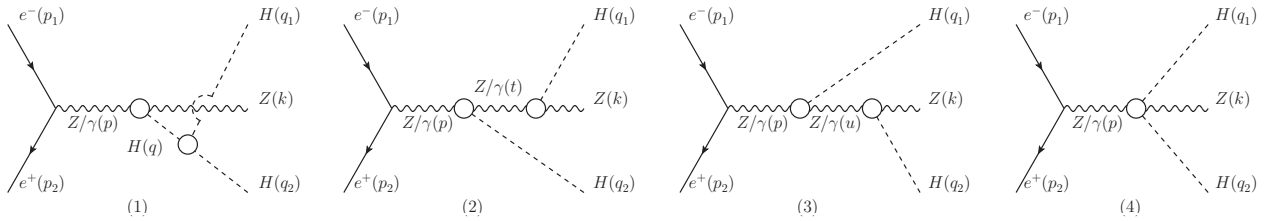


Figure 2: Feynman diagrams for $e^+e^- \to ZHH$ with our effective Lagrangian eq (5.1). The four-momentum of each particle is shown in parenthesis.

where E is the e^+e^- c.m. energy, w is the energy of the Z boson: $w = (E^2+m_Z^2-Q^2)/(2E)$ where $Q^2 = q\cdot q$, $-l$ is the momentum of the Z boson: $l = \sqrt{w^2-m_Z^2}$, and $q^\mu_{1,2}$ are the four-momenta of the two Higgs bosons. We parametrize $q^\mu_{1,2}$ in the rest frame of q^μ as

$$\begin{aligned} q^\mu &= (q_1+q_2)^\mu = (Q,0,0,0),\\ q_1^\mu &= \big(Q/2, r\sin\xi\cos\phi, r\sin\xi\sin\phi, r\cos\xi\big),\\ q_2^\mu &= \big(Q/2, -r\sin\xi\cos\phi, -r\sin\xi\sin\phi, -r\cos\xi\big), \end{aligned} \tag{2.2}$$

where $r = \sqrt{Q^2/4-m_H^2}$. Since we cannot distinguish the two Higgs bosons, we define the regions of the angles as $0\le\xi\le\pi/2$ and $0\le\phi\le 2\pi$ and identify the Higgs boson whose momentum along the z-axis is positive as the Higgs boson that has q_1^μ. The four-momenta $q^\mu_{1,2}$ in our e^+e^- c.m. frame can be easily obtained by a single boost along the positive direction of the z-axis:

$$q_1^\mu = \left(\frac{E-w}{2}+\frac{l}{Q}r\cos\xi, r\sin\xi\cos\phi, r\sin\xi\sin\phi, \frac{l}{2}+\frac{E-w}{Q}r\cos\xi\right), \tag{2.3a}$$

$$q_2^\mu = \left(\frac{E-w}{2}-\frac{l}{Q}r\cos\xi, -r\sin\xi\cos\phi, -r\sin\xi\sin\phi, \frac{l}{2}-\frac{E-w}{Q}r\cos\xi\right). \tag{2.3b}$$

We introduce the four-momenta t^μ and u^μ of the intermediate Z boson or the photon γ in the diagrams (2) and (3) of Figure 2, respectively:

$$\begin{aligned} t^\mu &= (k+q_1)^\mu\\ &= \left(\frac{E+w}{2}+\frac{l}{Q}r\cos\xi, r\sin\xi\cos\phi, r\sin\xi\sin\phi, -\frac{l}{2}+\frac{E-w}{Q}r\cos\xi\right),\\ u^\mu &= (k+q_2)^\mu\\ &= \left(\frac{E+w}{2}-\frac{l}{Q}r\cos\xi, -r\sin\xi\cos\phi, -r\sin\xi\sin\phi, -\frac{l}{2}-\frac{E-w}{Q}r\cos\xi\right). \end{aligned} \tag{2.4}$$

3 Differential cross section

We present an analytic expression for the differential cross section by assuming non-standard Higgs couplings. The effective Lagrangian, from which we obtain the Higgs couplings, will be given in Section 5. The Feynman diagrams contributing to the scattering amplitudes of the process $e^+e^- \to ZHH$ with our non-standard Higgs couplings are shown in Figure 2. It is an easy task to derive the scattering amplitudes in terms of the kinematic variables defined in Section 2. We find that the amplitude-squared summed over the Z boson helicity λ for a given electron helicity τ has the following form in the most general case:

$$\begin{aligned} \sum_{\lambda=\pm,0}|\mathcal{M}_\tau^\lambda|^2 =& F_1\big(1+\cos^2\Theta\big)+F_2\big(1-3\cos^2\Theta\big)+F_3\cos\Theta+F_4\sin\Theta\cos\phi+F_5\sin 2\Theta\cos\phi\\ &+F_6\sin^2\Theta\cos 2\phi+F_7\sin\Theta\sin\phi+F_8\sin 2\Theta\sin\phi+F_9\sin^2\Theta\sin 2\phi, \end{aligned} \tag{3.1}$$

where the Θ and ϕ dependences are completely factorized and the 9 functions F_i as the angular coefficients are independent on these two angles: $F_i = F_i(\tau,Q,\xi)$ [2]. The 9 functions F_i depend on

[2]The functions F_i depend on the e^+e^- c.m. energy (i.e. E in our notation), hence $F_i = F_i(\tau,Q,\xi,E)$ is the more appropriate expression. However, we regard E as a fixed value and do not write E explicitly in the arguments of functions throughout the paper.

the Higgs couplings. The 9 functions F_i can be experimentally determined by measuring the angles Θ and ϕ, therefore used to study the Higgs couplings. For an approach to isolate the functions, see eqs. (3.28) and (3.29) of ref. [38]. By means of eq. (3.1), the complete differential cross section for a given electron helicity τ is given by

$$\frac{d\sigma(\tau)}{d\Omega} \equiv \frac{d\sigma(\tau)}{d\cos\Theta dQ^2 d\cos\xi d\phi} = \frac{1}{1024\pi^4}\frac{l}{E^3}\sqrt{1-\frac{4m_H^2}{Q^2}}\sum_{\lambda=\pm,0}|\mathcal{M}_\tau^\lambda|^2. \tag{3.2}$$

By performing the integration over ϕ, we obtain the analytic form of the $\cos\Theta$ distribution:

$$\int_0^{2\pi} d\phi\frac{d\sigma(\tau)}{d\Omega} = \frac{1}{512\pi^3}\frac{l}{E^3}\sqrt{1-\frac{4m_H^2}{Q^2}}\Big[F_1\big(1+\cos^2\Theta\big)+F_2\big(1-3\cos^2\Theta\big)+F_3\cos\Theta\Big], \tag{3.3}$$

where the other 6 terms were eliminated by the integration. The numerical studies of the $\cos\Theta$ distribution in the literature e.g. [8,34] actually probe the 3 coefficients, which can be obtained by integrating eq. (3.3) over Q^2 and $\cos\xi$:

$$\begin{aligned}\frac{d\sigma(\tau)}{d\cos\Theta} &= \int_{4m_H^2}^{(E-m_Z)^2} dQ^2\int_0^1 d\cos\xi\int_0^{2\pi} d\phi\frac{d\sigma(\tau)}{d\Omega}\\ &= \int_{4m_H^2}^{(E-m_Z)^2} dQ^2\int_0^1 d\cos\xi\frac{1}{512\pi^3}\frac{l}{E^3}\sqrt{1-\frac{4m_H^2}{Q^2}}\Big[F_1\big(1+\cos^2\Theta\big)+F_2\big(1-3\cos^2\Theta\big)+F_3\cos\Theta\Big].\end{aligned} \tag{3.4}$$

By further integrating eq. (3.3) over $\cos\Theta$, we obtain

$$\frac{d\sigma(\tau)}{dQ^2 d\cos\xi} = \int_{-1}^1 d\cos\Theta\int_0^{2\pi} d\phi\frac{d\sigma(\tau)}{d\Omega} = \frac{1}{192\pi^3}\frac{l}{E^3}\sqrt{1-\frac{4m_H^2}{Q^2}}F_1, \tag{3.5}$$

where the other 2 terms were eliminated by the integration. From this, we can easily obtain the analytic form of the Q^2 distribution which has been numerically studied e.g. in refs. [9, 14] and that of the $\cos\xi$ distribution which ref. [7] mentions can be a good observable for measuring λ_H:

$$\frac{d\sigma(\tau)}{dQ^2} = \int_0^1 d\cos\xi\frac{1}{192\pi^3}\frac{l}{E^3}\sqrt{1-\frac{4m_H^2}{Q^2}}F_1, \tag{3.6a}$$

$$\frac{d\sigma(\tau)}{d\cos\xi} = \int_{4m_H^2}^{(E-m_Z)^2} dQ^2\frac{1}{192\pi^3}\frac{l}{E^3}\sqrt{1-\frac{4m_H^2}{Q^2}}F_1. \tag{3.6b}$$

The total cross section for a given electron helicity τ is given by

$$\sigma(\tau) = \int_{4m_H^2}^{(E-m_Z)^2} dQ^2\int_0^1 d\cos\xi\frac{1}{192\pi^3}\frac{l}{E^3}\sqrt{1-\frac{4m_H^2}{Q^2}}F_1. \tag{3.7}$$

We introduce the scaling variables

$$x_1 = \frac{2q_1^0}{E},\quad x_2 = \frac{2q_2^0}{E}. \tag{3.8}$$

Note that q_1^0 and q_2^0 are defined in eq. (2.3). By straightforward variable conversions in eq. (3.5), we obtain

$$\frac{d\sigma(\tau)}{dx_1 dx_2} = \frac{1}{192\pi^3}F_1 \tag{3.9}$$

which has been derived in refs. [25–27] and

$$\frac{d\sigma(\tau)}{dQ^2 d(t\cdot t)} = \frac{1}{192\pi^3 E^4}F_1 \tag{3.10}$$

which has been derived in ref. [33]. Note that the phase space region $0 \le \xi \le \pi/2$ (see below eq. (2.2) corresponds to $x_1 \ge x_2$ and $t\cdot t \ge u\cdot u$. The four-momenta t^μ and u^μ are defined in eq. (2.4). We emphasize that the observables which exist in the literature and are re-derived above in eqs. (3.6), (3.7), (3.9) and (3.10) are directly related to the function F_1, which is just one of the 9 functions in the differential cross section.

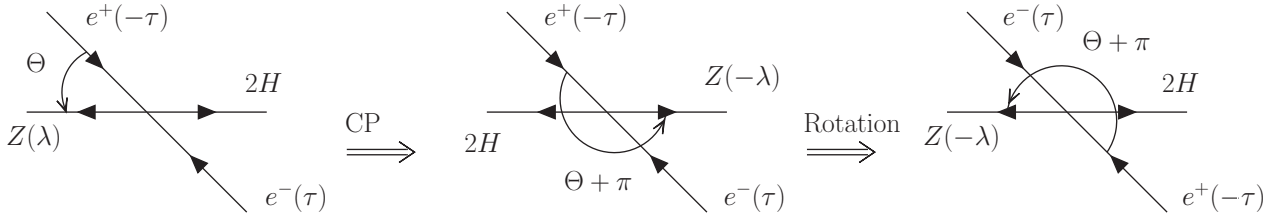


Figure 3: The states after the CP transformation are shown. At the second step, a rotation around the y-axis by π is performed. The helicity of each particle is shown in parenthesis.

4 Symmetry properties

The conditions imposed by symmetries lead to constraints on some of the 9 functions F_i. The picture in Figure 3 shows the original states and the states after the charge-conjugation (C) and parity (P) transformation. After the CP transformation, the states are simply rotated around the y-axis by π and we make the four-momentum q^μ come back to the original position. Note that we always have a freedom of performing 3-dimensional spatial rotations. While q^μ is unchanged, the four-momenta q_1^μ and q_2^μ are changed by the CP transformation and the rotation as

$$\begin{aligned} q_1^\mu &= \left(\frac{E-w}{2}+\frac{l}{Q}r\cos\xi, r\sin\xi\cos\phi, r\sin\xi\sin\phi, \frac{l}{2}+\frac{E-w}{Q}r\cos\xi\right), \\ &\xrightarrow[\text{CP}]{} \left(\frac{E-w}{2}+\frac{l}{Q}r\cos\xi, -r\sin\xi\cos\phi, -r\sin\xi\sin\phi, -\frac{l}{2}-\frac{E-w}{Q}r\cos\xi\right), \\ &\xrightarrow[\text{Rotation}]{} \left(\frac{E-w}{2}+\frac{l}{Q}r\cos\xi, r\sin\xi\cos\phi, -r\sin\xi\sin\phi, \frac{l}{2}+\frac{E-w}{Q}r\cos\xi\right). \end{aligned} \tag{4.1}$$

Notice that only the y-component of q_1^μ changes sign, which indicates that the azimuthal angle ϕ is $2\pi-\phi$ after the transformations. Therefore, CP invariance leads to the following relation for the differential cross section:

$$d\sigma(\tau,\Theta,Q,\xi,\phi) = d\sigma(\tau,\Theta+\pi,Q,\xi,2\pi-\phi), \tag{4.2}$$

where the one on the left hand side corresponds to the original states shown in the the left picture of Figure 3 and the one on the right hand side corresponds to the states after the CP transformation and the rotation shown in the the right picture of Figure 3. The explicit form of the right hand side of this equation is, from eqs. (3.1) and (3.2), given by

$$\begin{aligned} \frac{d\sigma(\tau)}{d\cos\Theta dQ^2 d\cos\xi d\phi} =& \frac{1}{1024\pi^4}\frac{l}{E^3}\sqrt{1-\frac{4m_H^2}{Q^2}}\Big[F_1\big(1+\cos^2\Theta\big)+F_2\big(1-3\cos^2\Theta\big)-F_3\cos\Theta \\ &-F_4\sin\Theta\cos\phi+F_5\sin 2\Theta\cos\phi+F_6\sin^2\Theta\cos 2\phi \\ &+F_7\sin\Theta\sin\phi-F_8\sin 2\Theta\sin\phi-F_9\sin^2\Theta\sin 2\phi\Big]. \end{aligned} \tag{4.3}$$

Let us remind that F_i are independent on Θ and ϕ, thus they have the same forms in the both sides of eq. (4.2) [3]. In eq. (4.3), we observe that the 4 terms of the 9 terms change sign. These terms, namely the F_3, F_4, F_8 and F_9 terms, are CP-odd. The 4 functions F_3, F_4, F_8 and F_9 must be zero if CP is conserved. In other words, observation of non-zero values in these 4 functions signals CP non-conservation.

Secondly, the picture in Figure 4 shows the original states and the states after the C, P and time-reversal transformation without interchanging the initial and final states (i.e. it does not reverse the time flow from the initial state to the final state). We denote it by $\widetilde{\text{T}}$. CP$\widetilde{\text{T}}$ invariance leads to the following relation for the differential cross section:

$$d\sigma(\tau,\Theta,Q,\xi,\phi) = d\sigma(\tau,\Theta+\pi,Q,\xi,\phi), \tag{4.4}$$

[3] We actually perform the rotation in order to make all of F_i invariant. Some of F_i are not invariant without the rotation. Even without the rotation, however, our conclusion that the F_3, F_4, F_8 and F_9 terms are CP-odd should remain the same, as long as physics is invariant under 3-dimensional spatial rotations.

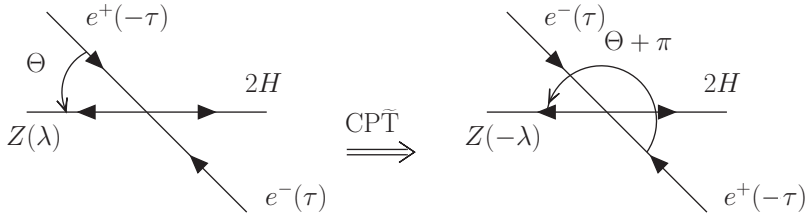


Figure 4: The states after the CP and time-reversal transformation without interchanging the initial and final states ($\widetilde{\mathrm{T}}$) are shown. The helicity of each particle is shown in parenthesis.

Functions	Symm. properties		beam pol.
	CP	$\mathrm{CP}\widetilde{\mathrm{T}}$	
F_1	+	+	-
F_2	+	+	-
F_3	−	−	∘
F_4	−	−	∘
F_5	+	+	-
F_6	+	+	-
F_7	+	−	∘
F_8	−	+	-
F_9	−	+	-

Table 1: Symmetry properties of the 9 functions in the differential cross section. The symbol + (−) means that the function is even (odd) under CP or $\mathrm{CP}\widetilde{\mathrm{T}}$. Observation of non-zero values in the CP-odd functions signals CP non-conservation. Observation of non-zero values in the $\mathrm{CP}\widetilde{\mathrm{T}}$-odd functions indicates the existence of re-scattering effects. The symbol ∘ in the last column indicates that the function can be suppressed without polarized e^+e^- beams.

where the one on the left hand side corresponds to the original states shown in the the left picture of Figure 4 and the one on the right hand side corresponds to the states after the $\mathrm{CP}\widetilde{\mathrm{T}}$ transformation shown in the right picture of Figure 4. The explicit form of the right hand side of this equation is, from eqs. (3.1) and (3.2), given by

$$\begin{aligned}\frac{d\sigma(\tau)}{d\cos\Theta dQ^2 d\cos\xi d\phi} =& \frac{1}{1024\pi^4}\frac{l}{E^3}\sqrt{1-\frac{4m_H^2}{Q^2}}\Big[F_1\big(1+\cos^2\Theta\big)+F_2\big(1-3\cos^2\Theta\big)-F_3\cos\Theta \\ &-F_4\sin\Theta\cos\phi+F_5\sin 2\Theta\cos\phi+F_6\sin^2\Theta\cos 2\phi \\ &-F_7\sin\Theta\sin\phi+F_8\sin 2\Theta\sin\phi+F_9\sin^2\Theta\sin 2\phi\Big],\end{aligned} \tag{4.5}$$

where we observe that the 3 terms of the 9 terms change sign. These terms, namely the F_3, F_4, and F_7 terms, are $\mathrm{CP}\widetilde{\mathrm{T}}$-odd. The 4 functions F_3, F_4, and F_7 must be zero if $\mathrm{CP}\widetilde{\mathrm{T}}$ is conserved. In other words, observation of non-zero values in these 3 functions signals $\mathrm{CP}\widetilde{\mathrm{T}}$ violation, which indicates the existence of re-scattering effects [36]. In Table 1, we summarize the symmetry properties of the functions. Notice that F_3 and F_4 are both CP-odd and $\mathrm{CP}\widetilde{\mathrm{T}}$-odd. Once we experimentally confirm that both the CP-odd functions (i.e. F_8 and F_9) and the $\mathrm{CP}\widetilde{\mathrm{T}}$-odd function (i.e. F_7) are small, we may ignore F_3 and F_4 since these are doubly suppressed.

5 Numerical studies

We obtain non-standard Higgs couplings to the Higgs boson itself, the Z boson and the photon γ from the following effective Lagrangian [39]:

$$\mathcal{L}_{\rm eff} = \big(1+\delta_1\big)m_Z^2\frac{H}{v}Z_\mu Z^\mu + \sum_{V=Z,A}\Big\{\delta_2^V\frac{H}{v}Z_{\mu\nu}V^{\mu\nu} + \delta_3^V\frac{1}{v}\big[(\partial^\mu H)Z^\nu - (\partial^\nu H)Z^\mu\big]V_{\mu\nu} + \tilde{\delta}_4^V\frac{H}{v}Z_{\mu\nu}\widetilde{V}^{\mu\nu}\Big\}$$
$$+ \big(1+\delta_5\big)m_Z^2\frac{H^2}{2v^2}Z_\mu Z^\mu + \sum_{V=Z,A}\Big\{\delta_6^V\frac{H^2}{2v^2}Z_{\mu\nu}V^{\mu\nu} + \delta_7^V\frac{H}{v^2}\big[(\partial^\mu H)Z^\nu - (\partial^\nu H)Z^\mu\big]V_{\mu\nu} + \tilde{\delta}_8^V\frac{H^2}{2v^2}Z_{\mu\nu}\widetilde{V}^{\mu\nu}\Big\}$$
$$+ \delta_2^{AA}\frac{H}{v}A_{\mu\nu}A^{\mu\nu} + \tilde{\delta}_4^{AA}\frac{H}{v}A_{\mu\nu}\widetilde{A}^{\mu\nu} - \frac{m_H^2}{2v}(1+\delta_9)H^3 + \delta_{10}\frac{H}{v}(\partial^\mu H)^2, \tag{5.1}$$

where $V_{\mu\nu} = \partial_\mu V_\nu - \partial_\nu V_\mu$, $\widetilde{V}^{\mu\nu} = \frac{1}{2}\epsilon^{\mu\nu\rho\sigma}V_{\rho\sigma}$ with our convention $\epsilon_{0123} = +1$, and v is the vacuum expectation value of the Higgs field: $v^{-2} = \sqrt{2}G_F$. All of the 18 coefficients δ_i are zero at the tree level in the SM. The 5 operators whose coefficients are $\tilde{\delta}_4^V$, $\tilde{\delta}_8^V$ and $\tilde{\delta}_4^{AA}$ are CP-odd and the other 13 operators are CP-even. If both the CP-even operator(s) and the CP-odd operator(s) exist, the theory is not CP conserving. If we consider the $SU(2)\times U(1)$ gauge invariant dimension six operators which consists of the gauge boson fields and the Higgs doublet field, there are 8 CP-even operators and 5 CP-odd operators [39, 40] which contribute to the Higgs couplings relevant to our process and their effects can be expressed as their contributions to our 18 coefficients δ_i. In addition, 2 CP-even operators affect our process through the renormalization of the SM parameters and the external Z and Higgs fields [39]. Feynman diagrams for the process $e^+e^- \to ZHH$ with this effective Lagrangian have been already shown in Figure 2. We have 12 diagrams maximum.

We integrate the differential cross section in eq. (3.2) over Q^2 and $\cos\xi$:

$$\frac{d\sigma(\tau)}{d\cos\Theta d\phi} = \mathcal{F}_1\big(1+\cos^2\Theta\big) + \mathcal{F}_2\big(1-3\cos^2\Theta\big) + \mathcal{F}_3\cos\Theta + \mathcal{F}_4\sin\Theta\cos\phi + \mathcal{F}_5\sin 2\Theta\cos\phi$$
$$+ \mathcal{F}_6\sin^2\Theta\cos 2\phi + \mathcal{F}_7\sin\Theta\sin\phi + \mathcal{F}_8\sin 2\Theta\sin\phi + \mathcal{F}_9\sin^2\Theta\sin 2\phi, \tag{5.2}$$

where

$$\mathcal{F}_i(\tau) = \int_{4m_H^2}^{(E-m_Z)^2} dQ^2\int_0^1 d\cos\xi\,\frac{1}{1024\pi^4}\frac{l}{E^3}\sqrt{1-\frac{4m_H^2}{Q^2}}F_i(\tau,Q,\xi). \tag{5.3}$$

Let us remind that the total cross section is directly related to $\mathcal{F}_1(\tau)$:

$$\sigma(\tau) = \frac{16}{3}\pi\mathcal{F}_1(\tau). \tag{5.4}$$

We assume unpolarized e^+e^- beams and define observables as

$$A_i \equiv \frac{\sum_\tau \mathcal{F}_i(\tau)}{\sum_\tau \mathcal{F}_1(\tau)}. \tag{5.5}$$

The symmetry property of A_i is the same as that of the corresponding function F_i. We note the advantages of the observables A_i:

- Some of systematic uncertainties such as the luminosity uncertainty cancel.
- We expect that $\mathcal{F}_i$ $(i = 2, 3, \cdots, 9)$ depend on the Higgs couplings in different ways from $\mathcal{F}_1$ (i.e. the total cross section) so that $\mathcal{F}_i$ $(i = 2, 3, \cdots, 9)$ provide us different information on the Higgs couplings. The observables A_i have the form that is sensitive to the difference between $\mathcal{F}_i$ $(i = 2, 3, \cdots, 9)$ and $\mathcal{F}_1$ in the dependence on the Higgs couplings.

For our numerical results, we set $E = 500$ GeV, $m_Z = 91.188$ GeV, $\Gamma_Z = 2.5$ GeV, $m_H = 125.5$ GeV, $\Gamma_H = 0$ GeV and $e = \sqrt{4\pi\alpha}$ with $\alpha = 1/128$. We assume that the Z boson and the Higgs bosons can be reconstructed. The phase space integration is performed with the program BASES [41].

We numerically study the dependence of A_i on the parameters in our effective Lagrangian. The single Higgs couplings to vector bosons such as HZZ may be precisely determined by measuring

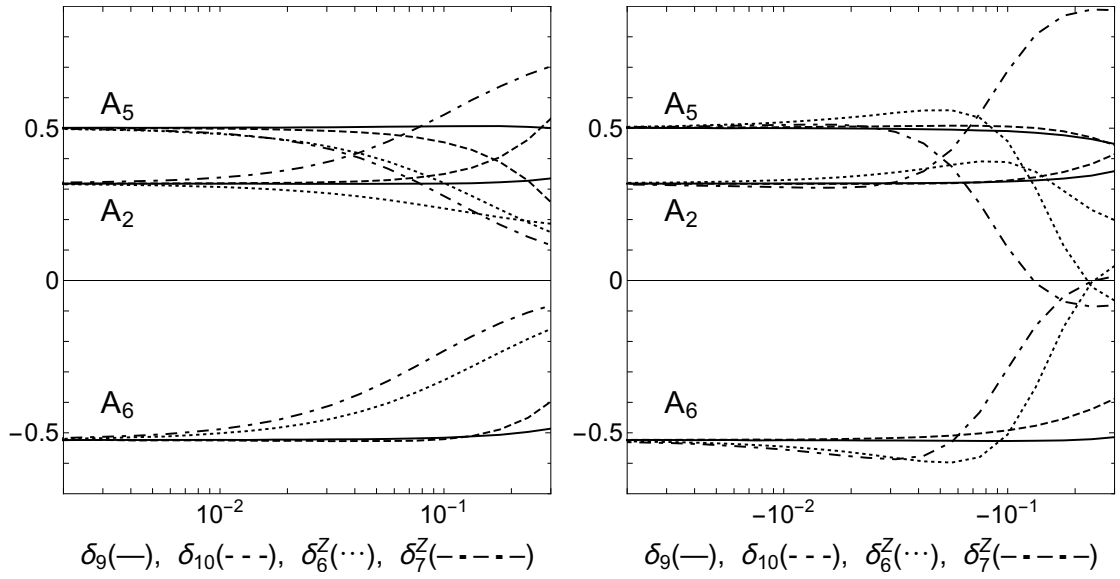


Figure 5: A_2, A_5 and A_6 are shown as deviations caused by adding non-zero parameters δ_9 (solid curve), δ_{10} (dashed curve), δ_6^Z (dotted curve) and δ_7^Z (broken curve). In the left panel the parameters take positive values, and in the right panel the parameters take negative values.

the polarization of the Z boson in the process $e^+e^- \to ZH$ [39, 42–44]. Therefore, we focus on the dependence on the parameters which cannot be accessed by single Higgs boson production processes. We choose as a benchmark point

$$\delta_2^Z = \delta_2^A = \delta_2^{AA} = -\delta_3^Z = -\delta_3^A = -0.05. \tag{5.6}$$

The other parameters are set zero. The total cross section with this choice is in agreement with the SM value within 10%. In Figure 5, the observables A_2, A_5 and A_6 are shown as deviations caused by adding non-zero parameters δ_9 (solid curve), δ_{10} (dashed curve), δ_6^Z (dotted curve) and δ_7^Z (broken curve). In the left panel the parameters take positive values, and in the right panel the parameters take negative values. The results show that $A_{2,5,6}$ depend little on δ_9. This indicates that $\mathcal{F}_{2,5,6}$ have the similar dependences on δ_9 as $\mathcal{F}_1$. The results also show that $A_{2,5,6}$ depend largely on δ_{10}, δ_6^Z and δ_7^Z. This indicates that the observables $\mathcal{F}_{2,5,6}$ depend on these parameters in different ways from the total cross section. In the left panel of Figure 6, the CP-odd observables A_8 and A_9 are shown as deviations caused by adding non-zero CP-odd parameters $\tilde{\delta}_8^Z$ (solid curve) and $\tilde{\delta}_8^Z = \tilde{\delta}_8^A$ (dashed curve). The results show that $A_{8,9}$ approach to zero as the CP-odd parameters become small, as expected. These observables are non-zero only when CP is violated. (Even if re-scattering effects exist, these observables are identically zero as long as CP is conserved.)

Due to the existence of the overall τ in the functions F_3, F_4 and F_7, the corresponding observables A_3, A_4 and A_7 can be suppressed. Longitudinally polarized e^+e^- beams will be useful to study these 3 functions. We define observables as

$$B_i \equiv \frac{(1+P_-)(1-P_+)\mathcal{F}_i(+) + (1-P_-)(1+P_+)\mathcal{F}_i(-)}{(1+P_-)(1-P_+)\mathcal{F}_1(+) + (1-P_-)(1+P_+)\mathcal{F}_1(-)}, \tag{5.7}$$

where P_- ($-1 \le P_- \le 1$) and P_+ ($-1 \le P_+ \le 1$) denote the degrees of longitudinal polarization of the electron and the positron, respectively. We choose $(P_-, P_+) = (-0.8, 0.3)$ [1]. In the right panel of Figure 6, the CP$\widetilde{\text{T}}$-odd observables A_7 and B_7 are shown as deviations caused by adding non-zero imaginary parts in the parameters δ_6^Z (solid curve) and δ_{10} (dashed curve) [4]. For the results in this panel, we choose as a benchmark point

$$\delta_2^Z = \delta_6^Z = -\delta_3^Z = -\delta_7^Z = \delta_{10} = 0.1, \tag{5.8}$$

and the other parameters are set zero. The total cross section with this choice is in agreement with the SM value within 30%. The results show that $B_7 > A_7$, i.e. the sensitivity to re-scattering

[4] Re-scattering effects can be approximately included by allowing imaginary parts in the Higgs couplings [36].

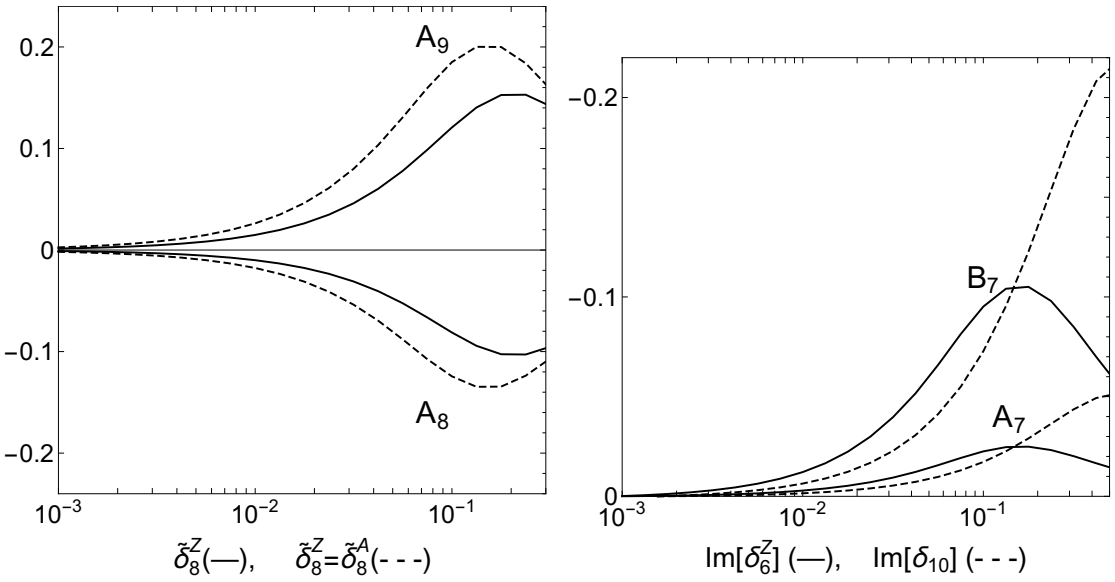


Figure 6: *Left:* CP-odd observables A_8 and A_9 are shown as deviations caused by adding non-zero parameters $\tilde{\delta}_8^Z$ (solid curve) and $\tilde{\delta}_8^Z = \tilde{\delta}_8^A$ (dashed curve). *Right:* CP$\widetilde{\text{T}}$-odd observables A_7 and B_7 are shown as deviations caused by adding non-zero imaginary parts in the parameters δ_6^Z (solid curve) and δ_{10} (dashed curve).

effects can be significantly increased by means of longitudinally polarized e^+e^- beams [5]. These observables are non-zero only when re-scattering effects exist. (Even if CP is violated, these observables are identically zero unless re-scattering effects exist.) Note that the SM predictions in these CP$\widetilde{\text{T}}$-odd observables are non-zero. The decay width in the Z boson propagators contributes to these observables, since it indeed reflects the re-scattering effect of the light fermions in the propagating Z boson. The contribution is, however, negligibly small as we can observe in our results (i.e. A_7 and B_7 approach to identically zero as the imaginary part of δ_6^Z or that of δ_{10} becomes small.).

6 Summary

In this paper, we have derived the analytic expression for the differential cross section that in the most general case has the 9 non-zero functions F_i $(i = 1, 2, \cdots, 9)$, for the process $e^+e^- \to ZHH$. The functions F_i are the coefficients of the 9 angular terms, depend on the Higgs couplings, and can be experimentally measured as observables. We have re-derived the analytic forms of the observables which exist in the literature and have been widely used. We have found that all of these observables are directly related to F_1, which is just one of our 9 functions. We have derived, for the first time, the analytic form of the Z boson polar angle Θ distribution, which is related to 3 of our 9 functions: F_1, F_2 and F_3. We have divided the 9 functions into 4 categories under CP and CP$\widetilde{\text{T}}$: 4 even-even (F_1, F_2, F_5, F_6), 1 even-odd (F_7), 2 odd-even (F_8, F_9) and 2 odd-odd (F_3, F_4). This result is summarized in Table 1.

We have introduced an effective Lagrangian for non-standard Higgs couplings to the Higgs boson itself, the Z boson and the photon, and numerically studied the dependence of $\mathcal{F}_i$ (this is obtained by integrating F_i over Q^2 and $\cos\xi$; see eq. (5.3)) on the parameters in the effective Lagrangian. For this purpose, we have formed new observables A_i and B_i (eqs. (5.5) and (5.7)) in terms of $\mathcal{F}_i$. These observables are defined in such way that the differences between $\mathcal{F}_i$ $(i = 2, 3, \cdots, 9)$ and $\mathcal{F}_1$ in the dependence on the Higgs couplings become apparent. Since $\mathcal{F}_1$ is directly related to the total cross section (eq. (5.4)), by means of A_i and B_i, we can learn whether $\mathcal{F}_i$ $(i = 2, 3, \cdots, 9)$ provide us different information about the Higgs couplings than the total cross section or not. We have found that the 3 observables $\mathcal{F}_{2,5,6}$ have the similar dependences on the constant shift of the trilinear self-coupling of the Higgs boson (i.e. δ_9 in eq. (5.1)) as the total cross section, while they have quite different dependences on the other CP-even parameters (i.e. δ_{10}, δ_6^Z and δ_7^Z)

[5] This benefit from polarized beams, however, becomes less clear when $HZ\gamma$, $H\gamma\gamma$ and/or $HHZ\gamma$ couplings are turned on, due to the interference between the diagrams exchanging the Z boson and those exchanging the photon.

than the total cross section. This is shown in Figure 5. The 2 CP-odd observables $\mathcal{F}_{8,9}$ and the CP$\widetilde{\text{T}}$-odd observable $\mathcal{F}_7$ clearly have advantages over the total cross section in determining CP-odd parameters and in observing re-scattering effects, respectively, since the total cross section is both CP-even and CP$\widetilde{\text{T}}$-even. We have shown that the CP-odd observables $\mathcal{F}_{8,9}$ directly measure CP violation, by showing that $\mathcal{F}_{8,9}$ approach to identically zero as the CP-odd parameters (i.e. $\tilde{\delta}_8^Z$ and $\tilde{\delta}_8^A$) become small. This is shown in the left panel of Figure 6. Finally, we have shown that the use of longitudinally polarized e^+e^- beams can enhance the ability of the CP$\widetilde{\text{T}}$-odd observable $\mathcal{F}_7$ which measures re-scattering effects. This is shown in the right panel of Figure 6.

Acknowledgments

I sincerely appreciate the support from the Alexander von Humboldt Foundation.

References

[1] H. Baer, T. Barklow, K. Fujii, Y. Gao, A. Hoang, S. Kanemura et al., *The International Linear Collider Technical Design Report - Volume 2: Physics*, 1306.6352.

[2] D. M. Asner et al., *ILC Higgs White Paper*, in *Proceedings, 2013 Community Summer Study on the Future of U.S. Particle Physics: Snowmass on the Mississippi (CSS2013): Minneapolis, MN, USA, July 29-August 6, 2013*, 2013. 1310.0763.

[3] A. Arbey et al., *Physics at the e+ e- Linear Collider*, *Eur. Phys. J.* **C75** (2015) 371, [1504.01726].

[4] K. Fujii et al., *Physics Case for the International Linear Collider*, 1506.05992.

[5] L. Linssen, A. Miyamoto, M. Stanitzki and H. Weerts, *Physics and Detectors at CLIC: CLIC Conceptual Design Report*, *ArXiv e-prints* (Feb., 2012) , [1202.5940].

[6] V. A. Ilyin, A. E. Pukhov, Y. Kurihara, Y. Shimizu and T. Kaneko, *Probing the H**3 vertex in e+ e-, gamma e and gamma gamma collisions for light and intermediate Higgs bosons*, *Phys. Rev.* **D54** (1996) 6717–6727, [hep-ph/9506326].

[7] F. Boudjema and E. Chopin, *Double Higgs production at the linear colliders and the probing of the Higgs selfcoupling*, *Z. Phys.* **C73** (1996) 85–110, [hep-ph/9507396].

[8] D. J. Miller and S. Moretti, *Can the trilinear Higgs selfcoupling be measured at future linear colliders?*, *Eur. Phys. J.* **C13** (2000) 459–470, [hep-ph/9906395].

[9] M. Battaglia, E. Boos and W.-M. Yao, *Studying the Higgs potential at the e+ e- linear collider*, *eConf* **C010630** (2001) E3016, [hep-ph/0111276].

[10] C. Castanier, P. Gay, P. Lutz and J. Orloff, *Higgs self coupling measurement in e+ e- collisions at center-of-mass energy of 500-GeV*, hep-ex/0101028.

[11] Y. Yasui, S. Kanemura, S. Kiyoura, K. Odagiri, Y. Okada, E. Senaha et al., *Measurement of the Higgs selfcoupling at JLC*, in *Linear colliders. Proceedings, International Workshop on physics and experiments with future electron-positron linear colliders, LCWS 2002, Seogwipo, Jeju Island, Korea, August 26-30, 2002*, pp. 112–114, 2002. hep-ph/0211047.

[12] Y. Takubo, *Analysis of ZHH in the 4-jet mode*, in *Linear colliders. Proceedings, International Linear Collider Workshop, LCWS08, and International Linear Collider Meeting, ILC08, Chicago, USA, Novermber 16-20, 2008*, 2009. 0901.3598.

[13] M. Faucci Giannelli, *Sensitivity to the Higgs Self-coupling Using the ZHH Channel*, in *Linear colliders. Proceedings, International Linear Collider Workshop, LCWS08, and International Linear Collider Meeting, ILC08, Chicago, USA, Novermber 16-20, 2008*, 2009. 0901.4895.

[14] U. Baur, *Measuring the Higgs Boson Self-coupling at High Energy e^+e^- Colliders*, *Phys. Rev.* **D80** (2009) 013012, [0906.0028].

[15] J. Tian, *Study of Higgs self-coupling at the ILC based on the full detector simulation at $\sqrt{s} = 500$ GeV and $\sqrt{s} = 1$ TeV*, in *Helmholtz Alliance Linear Collider Forum: Proceedings of the Workshops Hamburg, Munich, Hamburg 2010-2012, Germany*, (Hamburg), pp. 224–247, DESY, DESY, 2013.

[16] ILC Physics and Detector Study collaboration, J. Strube, *Measurement of the Higgs Boson Coupling to the Top Quark and the Higgs Boson Self-coupling at the ILC*, *Nucl. Part. Phys. Proc.* **273-275** (2016) 2463–2465.

[17] ATLAS collaboration, G. Aad et al., *Observation of a new particle in the search for the Standard Model Higgs boson with the ATLAS detector at the LHC*, *Phys. Lett.* **B716** (2012) 1–29, [1207.7214].

[18] CMS collaboration, S. Chatrchyan et al., *Observation of a new boson at a mass of 125 GeV with the CMS experiment at the LHC*, *Phys. Lett.* **B716** (2012) 30–61, [1207.7235].

[19] G. J. Gounaris, D. Schildknecht and F. M. Renard, *Test of Higgs Boson Nature in $e^+e^- \to HHZ$*, *Phys. Lett.* **83B** (1979) 191.

[20] V. D. Barger, T. Han and R. J. N. Phillips, *Double Higgs Boson Bremsstrahlung From W and Z Bosons at Supercolliders*, *Phys. Rev.* **D38** (1988) 2766.

[21] Q.-H. Dai, W.-G. Ma and Y.-Y. Liu, *TEST OF HIGGS COUPLINGS IN E+ E- COLLIDERS*, *Phys. Lett.* **B226** (1989) 180–184.

[22] R.-Y. Zhang, W.-G. Ma, H. Chen, Y.-B. Sun and H.-S. Hou, *Full O(alpha(ew)) electroweak corrections to e+ e- —¿ H H Z*, *Phys. Lett.* **B578** (2004) 349–358, [hep-ph/0308203].

[23] G. Belanger, F. Boudjema, J. Fujimoto, T. Ishikawa, T. Kaneko, Y. Kurihara et al., *Full 0(alpha) electroweak corrections to double Higgs strahlung at the linear collider*, *Phys. Lett.* **B576** (2003) 152–164, [hep-ph/0309010].

[24] J.-i. Kamoshita, Y. Okada, M. Tanaka and I. Watanabe, *Studying the Higgs potential via e+ e- —¿ Z h h*, in *Physics and experiments with linear colliders. Proceedings, 3rd Workshop, Morioka-Appi, Japan, September 8-12, 1995. Vol. 1, 2*, pp. 418–427, 1996. hep-ph/9602224.

[25] A. Djouadi, H. E. Haber and P. M. Zerwas, *Multiple production of MSSM neutral Higgs bosons at high-energy e+ e- colliders*, *Phys. Lett.* **B375** (1996) 203–212, [hep-ph/9602234].

[26] P. Osland and P. N. Pandita, *Measuring the trilinear couplings of MSSM neutral Higgs bosons at high-energy e+ e- colliders*, *Phys. Rev.* **D59** (1999) 055013, [hep-ph/9806351].

[27] A. Djouadi, W. Kilian, M. Muhlleitner and P. M. Zerwas, *Testing Higgs selfcouplings at e+ e- linear colliders*, *Eur. Phys. J.* **C10** (1999) 27–43, [hep-ph/9903229].

[28] A. Djouadi, *The Higgs sector of supersymmetric theories and the implications for high-energy colliders*, *Eur. Phys. J.* **C59** (2009) 389–426, [0810.2439].

[29] R. Grber and M. Mhlleitner, *Higgs Pair Production in Composite Higgs Models at the ILC*, in *Helmholtz Alliance Linear Collider Forum: Proceedings of the Workshops Hamburg, Munich, Hamburg 2010-2012, Germany*, (Hamburg), pp. 352–363, DESY, DESY, 2013.

[30] S. Kanemura, K. Kaneta, N. Machida, S. Odori and T. Shindou, *Single and double production of the Higgs boson at hadron and lepton colliders in minimal composite Higgs models*, *Phys. Rev.* **D94** (2016) 015028, [1603.05588].

[31] E. Asakawa, D. Harada, S. Kanemura, Y. Okada and K. Tsumura, *Higgs boson pair production in new physics models at hadron, lepton, and photon colliders*, *Phys. Rev.* **D82** (2010) 115002, [1009.4670].

[32] V. Barger, T. Han, P. Langacker, B. McElrath and P. Zerwas, *Effects of genuine dimension-six Higgs operators*, *Phys. Rev.* **D67** (2003) 115001, [hep-ph/0301097].

[33] R. Contino, C. Grojean, D. Pappadopulo, R. Rattazzi and A. Thamm, *Strong Higgs Interactions at a Linear Collider*, *JHEP* **02** (2014) 006, [1309.7038].

[34] S. Kumar and P. Poulose, *Influence of anomalous VVH and VVHH on determination of Higgs self couplings at ILC*, 1408.3563.

[35] T. Barklow, K. Fujii, S. Jung, M. E. Peskin and J. Tian, *Model-Independent Determination of the Triple Higgs Coupling at e+e- Colliders*, 1708.09079.

[36] K. Hagiwara, R. D. Peccei, D. Zeppenfeld and K. Hikasa, *Probing the Weak Boson Sector in $e^+e^- \to W^+W^-$*, *Nucl. Phys.* **B282** (1987) 253–307.

[37] D. Binosi and L. Theussl, *JaxoDraw: A Graphical user interface for drawing Feynman diagrams*, *Comput. Phys. Commun.* **161** (2004) 76–86, [hep-ph/0309015].

[38] J. Nakamura, *Polarisations of the Z and W bosons in the processes $pp \to ZH$ and $pp \to W^{\pm}H$*, *JHEP* **08** (2017) 008, [1706.01816].

[39] K. Hagiwara and M. L. Stong, *Probing the scalar sector in e+ e- —¿ f anti-f H*, *Z. Phys.* **C62** (1994) 99–108, [hep-ph/9309248].

[40] K. Hagiwara, S. Ishihara, R. Szalapski and D. Zeppenfeld, *Low-energy effects of new interactions in the electroweak boson sector*, *Phys. Rev.* **D48** (1993) 2182–2203.

[41] S. Kawabata, *A New version of the multidimensional integration and event generation package BASES/SPRING*, *Comput. Phys. Commun.* **88** (1995) 309–326.

[42] R. Rattazzi, *Anomalous Interactions at the Z^0 Pole*, *Z. Phys.* **C40** (1988) 605–611.

[43] V. D. Barger, K.-m. Cheung, A. Djouadi, B. A. Kniehl and P. M. Zerwas, *Higgs bosons: Intermediate mass range at e+ e- colliders*, *Phys. Rev.* **D49** (1994) 79–90, [hep-ph/9306270].

[44] K. Hagiwara, S. Ishihara, J. Kamoshita and B. A. Kniehl, *Prospects of measuring general Higgs couplings at e+ e- linear colliders*, *Eur. Phys. J.* **C14** (2000) 457–468, [hep-ph/0002043].